ELSEVIER

Retrieval of the aerosol particle size distribution function by incorporating *a priori* information

Yanfei Wang[a, b, *], Shufang Fan[c], Xue Feng[d]

[a] *Institute of Geology and Geophysics, Chinese Academy of Sciences, P.O. Box 9825, Beijing 100029, PR China*
[b] *State Key Laboratory of Remote Sensing Science, Jointly Sponsored by the Institute of Remote Sensing Applications of Chinese Academy of Sciences and Beijing Normal University, Beijing 100101, PR China*
[c] *Department of Mathematics, Liaocheng University, Shandong 252059, PR China*
[d] *School of Geography, Beijing Normal University, Beijing 100875, PR China*

Abstract

The determination of the aerosol particle size distribution function using the particle spectrum extinction equation is an ill-posed integral equation of the first kind. To overcome the ill-posedness, regularization techniques such as Phillips–Twomey's regularization, Tikhonov's smooth regularization as well as some iterative methods were developed. However, most of the literature focuses on improving the solvability of the problem without introducing some useful *a priori* information, which are essential to ill-posed inverse problems, since it is known that, we are often faced with limited/insufficient observations in remote sensing. Therefore, we restudy this problem. We first formulate the problem in l^1 space and solve a nonnegative constrained problem to obtain a useful *a priori* solution, then we use this solution to reformulate the problem in l^2 space and solve a regularized problem. Numerical results are based on the remotely sensed data by Sun-photometer CE 318 for Poyang lake region of Jiangxi Province and are performed to show the efficiency and feasibility of the proposed algorithms.
© 2007 Elsevier Ltd. All rights reserved.

1. Introduction

Aerosol is a suspension of small solid or liquid particles in the atmosphere, which plays an important role in the environment since they take part in many physical and chemical processes (Bohren & Huffman, 1983; Davies, 1974; Mccartney, 1976; Twomey, 1977). It is well known that the characteristics of the aerosol particle size, which can be represented as a size distribution function in the mathematical formalism, say $n(r)$, plays an important role in affecting the climate. So, it is necessary to determine the size distribution function of the aerosol particles. Since the relationship between the size of atmospheric aerosol particles and the wavelength dependence of the extinction coefficient was

---

* Corresponding author. Institute of Geology and Geophysics, Chinese Academy of Sciences, P.O. Box 9825, Beijing 100029, PR China.
Tel.: +86 10 6200 8008; fax: +86 10 6201 0846.
E-mail address: yfwang_ucf@yahoo.com (Y. Wang).

first suggested by Ångström (1929), the size distribution began to be retrieved from extinction measurements. First, Ångström inferred that the parameters of a Junge size distribution could be obtained from the aerosol optical thickness (AOT) at multiple wavelengths and obtained the useful Ångström empirical formula of the Junge size distribution, $\tau_{aero} = \beta\lambda^{-\alpha}$, where τ_{aero} is the AOT, β is the turbidity coefficient, and α is the Ångström exponent reflecting the aerosol size distribution.

The attenuation by aerosols can be written as an integral equation of the first kind

$$\tau_{aero}(\lambda) = \int_0^\infty \pi r^2 Q_{ext}(r, \lambda, \eta) n(r)\, \mathrm{d}r + \varrho(\lambda), \tag{1}$$

where r is the particle radius; $n(r)$ is the columnar aerosol size distribution (i.e., the number of particles per unit area per unit radius interval in a vertical column through the atmosphere); η is the complex refractive index of the aerosol particles; λ is the wavelength; $\varrho(\lambda)$ is the error/noise and $Q_{ext}(r, \lambda, \eta)$ is the extinction efficiency factor from Mie theory. Since AOT can be obtained from the measurements of the solar flux density with Sun-photometers, one can retrieve the size distribution by the inversion of AOT measurements through the above equations. This type of method is called extinction spectrometry, which is not only the earliest method applying remote sensing to determine atmospheric aerosol size characteristics but also the most matured method so far.

To overcome the oscillations in recovering the particle size distribution function $n(r)$, various techniques have been applied, e.g., Phillips–Twomey's second difference method (Phillips, 1962; Twomey, 1963, 1975), regularization by truncated singular value decomposition for LIDAR data (Bockmann, 2001), linear and nonlinear iterative techniques (Chahine, 1970; Ferri, Bassini, & Paganini, 1995; Lumme & Rahola, 1994; Twomey, 1975; Yamamoto & Tanaka, 1969), Tikhonov's smooth regularization (Wang, Fan, Feng, Yan, & Guan, 2006), genetic algorithms (Ye et al., 1999), moments methods (Heintzenberg, 1994; Wright, 2000; Wright et al., 2002) and computed tomography (Ramachandran, Leith, & Todd, 1994). However, all of the methods do not consider how to incorporate useful *a priori* information from the infinite solution space because the practical observations are insufficient due to the limitations of the devices. This paper will address this problem and propose a useful retrieval method. Numerical experiments based on the Sun-photometer CE 318 were performed to show the efficiency of the proposed solution methods.

The structure of the paper is organized as follows: Section 2 introduces the experimental site in this study and the Sun-photometer specifications. Section 3 provides the methodology for the problem formulation in functional and finite spaces. In Section 4.1, an efficient *a priori* solution in l^1 space is presented, and an interior point solution method is proposed; in Section 4.2, the damped Gauss–Newton method is described, and its regularization involving *a priori* information is addressed in Section 4.3. In Section 4.4, the aerosol particle size distribution function retrieval problem by the proposed method is addressed. Also a geometric *a posteriori* regularization parameter choice method is introduced. In Section 5, we first perform theoretical simulations; then we use the ground-based remotely sensed measurements to verify the numerical results. In Section 6, some concluding remarks are given. Finally, we provide appendices which list basic information about the conception of "*a priori*" and "regularization", the computation of *a priori* by an interior-point solution method and the Wolfe line search for damped Gauss–Newton method.

Throughout the paper, we use the following notations: ":=" denotes "defined as", "$\vec{n}$" denotes the discretization of a function n, "argmax" and "argmin" denote "maximization for an argument" and "minimization for an argument", respectively, "max" and "min" denote "maximizing" and "minimizing" some functional, respectively, $A^\dagger$ denotes the (Moore-Penrose) generalized inverse, "A^T" denotes the transpose of matrix A and "diag($\cdot$)" denotes a diagonal matrix.

2. Experimental site and instrument specifications

The investigations were carried out in October, 2005. The test area in this study is Yingtan city which is located in Poyang lake region of Jiangxi Province in China. It is a typical test region in many applications. The altitude and the pressure of Yingtan city average 45.2 m and 1013.4 hPa, respectively, the relative humidity averages 74%, the wind speed varies from 0.3 to 3.3 m/s. We performed the data measurement in a region which is located in the longitude $116°55'33.7''$ east of Greenwich, latitude $28°12'30''$ north. It is noted that Yingtan city is not a big city, the traffic may not cause either the local air pollution or the thermal and humidity regimes in the atmosphere of the measurement area.

The Sun-photometer for measuring the attenuation of aerosols is CE 318 which is illustrated in Wang et al. (2006). It has four aerosol channels: 440, 670, 870, and 1020 nm, which can be used for estimating AOT. The instrument automatically computes the position of the Sun and tracks its movement and is also useful for the atmospheric correction

of remote sensing data. Since the CE 318 can only supply four aerosol channels, only four observations are obtained, which are insufficient for the retrieval of the particle size distribution function $n(r)$ by solving Eq. (1). Therefore, numerical difficulty occurs.

3. Problem formulation

The general formulation of inversion schemes using operator theory in functional space is briefly described and illustrated in finite space.

3.1. Operator equations of the first kind

A common feature for all particle size distribution measurement systems is that the relation between noiseless observations and the size distribution function can be expressed as a first kind Fredholm integral equation (Nguyen & Cox, 1989; Shifrin & Zolotov, 1996; Twomey, 1975; Voutilainenand & Kaipio, 2000; Wang, 2007)

$$\int_a^b k(x, y)n(y)\, \mathrm{d}y = o(x),\tag{2}$$

where $[a, b]$ is the integral interval which characterizes the lower and upper limits of the size range of interests, $o(x)$ is an error-free observation, $x = \log r$ and $k(x, y)$ is a weight function (or more generally, the kernel function) that characterizes the classification, losses and detection properties of the measurement system.

The observations are usually contaminated by noise. Hence, relation (2) between the observation $o(x)$ and the size distribution $n(x)$ is

$$\int_a^b k(x, y)n(y)\, \mathrm{d}y + \varrho(x) = o(x) + \varrho(x) = d(x),\tag{3}$$

where $\varrho(x)$ is the unknown observation error. Therefore, the inverse problem is to solve a perturbed Fredholm integral equation of the first kind to get the size distribution $n(x)$.

Let us rewrite Eq. (1) in the form of the abstract operator equation

$$\begin{aligned} K : F &\longrightarrow O, \\ (Kn)(\lambda) + \varrho(\lambda) &= d(\lambda), \end{aligned}\tag{4}$$

where $(Kn)(\lambda) := \int_0^\infty k(r, \lambda, \eta)n(r)\, \mathrm{d}r$; $k(r, \lambda, \eta) = \pi r^2 Q_{\text{ext}}(r, \lambda, \eta)$; F denotes the function space of aerosol size distributions; and O denotes the observation space. Both F and O are considered to be separable Hilbert spaces. Note that $\tau_{\text{aero}}(\lambda)$ in Eq. (1) is the measured term, and it inevitably induces noise/errors. Hence, $d(\lambda)$ is a perturbed right-hand side. Using operator symbol, Eq. (4) can be written as

$$Kn + \varrho = d.\tag{5}$$

3.2. Discrete formulation in finite spaces

Note that Eq. (4) is an infinite dimensional problem with only a finite set of observations, so it is improbable to implement such a system by computer to get a continuous expression of the size distribution $n(r)$. Using collocation (Wang et al., 2006), the infinite problem can be written in a finite dimensional form by sampling some grids $\{r_j\}_{j=1}^N$ in the interval of interests $[a, b]$.

Denoting by $\mathscr{K} = (\mathscr{K}_{ij})_{M \times N}$, $\vec{n}$, $\vec{\varrho}$ and $\vec{d}$ the corresponding vectors, we have

$$\mathscr{K}\vec{n} + \vec{\varrho} = \vec{d}.\tag{6}$$

This discrete form can be used for computer simulations.

4. Theoretical development

4.1. Solving for an efficient a priori information in l^1 space

It is clear that when the number of observations is insufficient, the inversion of Eq. (4) is ill-posed. The ill-posedness occurs not only for the instability driven by the small algebraic characteristic spectrum but also for choosing a suitable solution from the solution set that consists of infinite solutions.

The ill-posedness is an intrinsic feature of the inverse problem. Unless some additional information is imposed, such as monotonicity, smoothness, boundedness or the error bound of the raw data, the difficulty is hard to be resolved. As is pointed out in Xiao, Yu, and Wang (2003) that, a lack of information cannot be remedied by any mathematical trickery. However, we can retrieve most of the information of the original problem by some kind of regularization. The regularization mentioned here, means that the solution can be found by replacing the original problem with a well-posed problem. One of the techniques is the improvement of the solvability by extension of the solution space, which will be presented in the following paragraph; another technique is seeking an optimized solution of a variational problem.

The particle size distribution function of aerosols is always nonnegative. Therefore, to extend the solution space, we solve an l^1 norm problem

$$\min \|\vec{n}\|_{l^1} \quad \text{subject to } \mathcal{K}\vec{n} = \vec{d}, \ \ \vec{n} \geqslant 0. \tag{7}$$

It is clear that Eq. (7) is equivalent to

$$\min e^{\mathrm{T}}\vec{n} \quad \text{subject to } \mathcal{K}\vec{n} = \vec{d}, \ \ \vec{n} \geqslant 0, \tag{8}$$

where e is a vector with all components 1. Then the optimal solution of problem (8) is also a solution of problem (7). So the remaining task is to solve Eq. (8) efficiently.

The l^1 norm solution method seeks a feasible solution within the feasible set

$$S = \{\vec{n} : \mathcal{K}\vec{n} = \vec{d}, \vec{n} \geqslant 0\}.$$

It is actually searching for an interior point within the feasible set S; it is called the interior point method (Ye, 1997). The dual standard form of Eq. (8) is in the form

$$\max \vec{d}^{\mathrm{T}}\vec{z} \quad \text{subject to } s = e - \mathcal{K}^{\mathrm{T}}\vec{z} \geqslant 0. \tag{9}$$

Therefore, the optimality conditions for $(\vec{n}, \vec{z}, s)$ to be a primal–dual solution triplet are

$$\mathcal{K}\vec{n} = \vec{d}, \tag{10}$$
$$\mathcal{K}^{\mathrm{T}}\vec{z} + s = e, \tag{11}$$
$$\tilde{S}\tilde{F}e = 0, \tag{12}$$
$$\vec{n} \geqslant 0, \quad s \geqslant 0, \tag{13}$$

where

$$\tilde{S} = \mathrm{diag}(s_1, s_2, \ldots, s_N), \quad \tilde{F} = \mathrm{diag}(n_1, n_2, \ldots, n_N).$$

The notation $\mathrm{diag}(\cdot)$ denotes the diagonal matrix whose only nonzero components are the main diagonal line.

The interior point method generates iteration points $\{\vec{n}_k, \vec{z}_k, s_k\}$ such that $\vec{n}_k > 0$ and $s_k > 0$. As the iteration index k approaches infinity, the equality-constraint violations $\|\vec{d} - \mathcal{K}\vec{n}_k\|$ and $\|\mathcal{K}^{\mathrm{T}}\vec{z}_k + s_k - e\|$ and the duality gap $\vec{n}_k^{\mathrm{T}}s_k$ are driven to zero, yielding a limiting point that solves the primal and dual linear problems.

Primal–dual methods are a variant of Newton's method applied to the system of equations formed by the optimality conditions, Eqs. (10)–(12). Given the current iteration point $[\vec{n}_k, \vec{z}_k, s_k]^{\mathrm{T}}$ and the damping parameter $\beta_k \in [0, 1]$, the

search direction $[\Delta_{\vec{n}}, \Delta_{\vec{z}}, \Delta_s]$ is generated by solving the linear system

$$
\begin{bmatrix} \mathscr{K} & 0 & 0 \\ 0 & \mathscr{K}^{\mathrm{T}} & I \\ \tilde{S}_k & 0 & \tilde{F}_k \end{bmatrix} \begin{bmatrix} \Delta_{\vec{n}} \\ \Delta_{\vec{z}} \\ \Delta_s \end{bmatrix} = \begin{bmatrix} \vec{d} - \mathscr{K}\vec{n}_k \\ e - \mathscr{K}^{\mathrm{T}}\vec{z}_k - s_k \\ \beta_k \mu_k e - \tilde{S}_k \tilde{F}_k e \end{bmatrix},
\tag{14}
$$

where $\beta_k = (1/N)\vec{n}_k^{\mathrm{T}} s_k$. Choosing the step size τ_k to retain the positivity of $\vec{n}$ and s, and step to a new point

$$
\vec{n}_{k+1} := \vec{n}_k + \tau_k \Delta_{\vec{n}}, \quad \vec{z}_{k+1} := \vec{z}_k + \tau_k \Delta_{\vec{z}}, \quad s_{k+1} := s_k + \tau_k \Delta_s.
\tag{15}
$$

The solution $\vec{n}$ denoted by $\vec{n}_0$, as an *a priori* information, will be used in the iterative regularization process.

4.2. Damped Gauss–Newton method

Denoting by $R(\vec{n}) = \mathscr{K}\vec{n} - \vec{d}$, we consider the functional in l^2 space

$$
J[\vec{n}] = \|R(\vec{n})\|_{l^2}^2.
\tag{16}
$$

It is easy to see that the gradient and Hessian of $J[\vec{n}]$ are, respectively, given by

$$
g(\vec{n}) = \mathscr{K}^{\mathrm{T}}(\mathscr{K}\vec{n} - \vec{d}), \quad H = \mathscr{K}^{\mathrm{T}}\mathscr{K}.
\tag{17}
$$

The Gauss–Newton method computes a step $s_k = \vec{n}_{k+1} - \vec{n}_k$ by

$$
\min \tfrac{1}{2}\|R(\vec{n}_k) + R'(\vec{n}_k)s\|^2,
\tag{18}
$$

which leads to the solution

$$
s_k = -R'(\vec{n}_k)^{\dagger} g_k = -H^{-1}g_k,
\tag{19}
$$

$$
\vec{n}_{k+1} = \vec{n}_k + s_k,
\tag{20}
$$

where $g_k = g(\vec{n}_k)$.

In the damped Gauss–Newton method in each iteration a line search technique is used to ensure a decreased direction, i.e.,

$$
s_k = -\gamma_k H^{-1}g_k,
\tag{21}
$$

where γ_k is obtained by solving one-dimensional nonlinear optimization problem

$$
\gamma_k = \mathrm{argmin}_{\gamma}\, \phi(\gamma) := J[\vec{n}_k + \gamma s_k].
\tag{22}
$$

In our calculation, the Wolfe line search technique is used (see Appendix D for details).

However, due to the rank deficiency of H the problem is ill-posed and is quite difficult to solve; therefore, regularization is necessary to tackle the ill-posedness.

4.3. Regularization by incorporating an efficient a priori information

A regularized damped Gauss–Newton method refers to computing a Gauss–Newton step s_k by

$$
s_k = -\gamma_k (H + \alpha_k L)^{-1} g_k,
\tag{23}
$$

where L is a smooth matrix which can be chosen by users, α_k is the regularization parameter. However, this regularization does not contain any information about the solution. We consider an *a priori* information-imposed method

$$
s_k = -\gamma_k (H + \alpha_k L)^{-1}(g_k + \alpha_k(\vec{n}_k - \vec{n}_0)),
\tag{24}
$$

where $\vec{n}_0$ is the so-called *a priori* information about the solution $\vec{n}$. The convergence theory and methods have been thoroughly investigated by Bakushinsky and Goncharsky (1994).

4.4. Aerosol particle size distribution function retrieval

To retrieve the aerosol particle size distribution function $n(r)$, we need to solve Eqs. (7) and (24) for the AOT at different wavelengths. We are interested in the particle size in the interval [0.1, 10] μm. A coarse difference gridding ($N \leqslant 20$) induces large quadrature errors; therefore, we choose a relatively large difference gridding, $N = 200$.

To perform the numerical computation, we apply the technique developed in King, Byrne, Herman, and Reagan (1978), that is, we assume that the actual aerosol particle size distribution function consists of the multiplication of two functions $h(r)$ and $f(f) : n(r) = h(r) f(r)$, where $h(r)$ is a rapidly varying function of r, while $f(r)$ is more slowly varying. In this way we have

$$\tau_{\text{aero}}(\lambda) = \int_a^b [k(r, \lambda, \eta) h(r)] f(r) \, dr, \tag{25}$$

where $k(r, \lambda, \eta) = \pi r^2 Q_{\text{ext}}(r, \lambda, \eta)$ and $k(r, \lambda, \eta) h(r)$ is the new kernel function corresponding to a new operator Ξ:

$$(\Xi f)(r) = \tau_{\text{aero}}(\lambda). \tag{26}$$

The discretization of Ξ is again denoted by the matrix $\mathcal{K}$.

Selection of the regularization parameter α is also a major issue in numerical computation. In theory, α can neither be too large nor be too small. A larger α yields a well-posed problem but the solution is far away from the true value. Whereas a smaller α yields a better approximation but with large instabilities. Therefore, a trade-off must be found to balance the ill-posed nature of the discrete matrix $\mathcal{K}$. There are two types of parameter selection methods: an *a priori* way and an *a posteriori* way. For *a priori* choice of the regularization parameter, α should be limited to within $(0, 1)$. Since the error or noise level δ is not always to be estimated, we will not apply the *a posteriori* technique developed in Wang et al. (2006). Instead, we choose the regularization parameter α in a geometric manner:

$$\alpha_k = \alpha_0 \cdot \xi^{k-1}, \tag{27}$$

where $\alpha_0 \in (0, 1)$ which can be provided by the user, for example, $\alpha_0 = 0.1$; $\xi \in (0, 1)$ is the factor of proportionality and k is the kth iteration. It is quite natural to use this parameter selection rule, since in theory, α_k should approach zero as k approaches infinity.

The smooth matrix L is chosen as a triangular matrix in the form

$$L = \begin{bmatrix} 1 + \dfrac{1}{h_r^2} & -\dfrac{1}{h_r^2} & 0 & \cdots & 0 \\[2ex] -\dfrac{1}{h_r^2} & 1 + \dfrac{2}{h_r^2} & -\dfrac{1}{h_r^2} & \cdots & 0 \\[2ex] \vdots & \ddots & \ddots & \ddots & \vdots \\[2ex] 0 & \cdots & -\dfrac{1}{h_r^2} & 1 + \dfrac{2}{h_r^2} & -\dfrac{1}{h_r^2} \\[2ex] 0 & \cdots & 0 & -\dfrac{1}{h_r^2} & 1 + \dfrac{1}{h_r^2} \end{bmatrix}, \tag{28}$$

where h_r is the step size of the grids in $[a, b]$, which can be equidistant if $h_r = (b - a)/(N - 1)$, or different if h_r is variable or adaptive. This matrix is shown to be effective in stabilizing oscillations of the solution (Wang et al., 2006).

For the solution of the linear matrix-vector equation, Eq. (24), we use the Cholesky decomposition method. This method is stable for finding a solution from a symmetric definite system with smaller computational cost $O(\frac{1}{6} N^3)$.

5. Numerical experiments

5.1. Theoretical simulation

To verify the feasibility of our inversion method, we have tested it by computer simulations. The simulation consists of two steps. First, a simulated extinction signal (input signal) is generated by computer according to Eq. (3) for a given
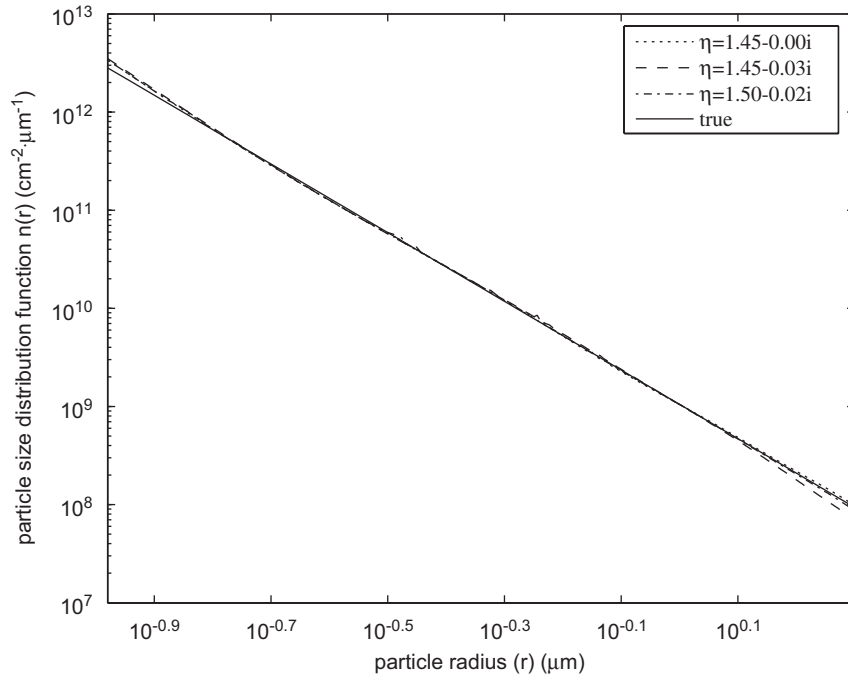
Fig. 1. Input and retrieved results with our inversion method in the case of error level $\delta = 0.005$ and different complex refractive indices.

number of particle size distribution $n_{\text{true}}(r)$ (input distribution) and for a given complex refractive index η. Then, the input signal is processed through our algorithm, and the retrieved distribution is compared with input one.

In practice, an exact discretization form $\vec{o}$ of the right-hand side of Eq. (2) cannot be obtained accurately; instead a perturbed version $\vec{d}$ is obtained. Numerically, a vector $\vec{d}$ should contain different kind of noises. Here, for simplicity, we assume that the noise is additive, and is mainly the Gaussian random noise, that is, we have

$$\vec{d} = \vec{o} + \delta \cdot \text{rand}(\text{size}(\vec{o})), \tag{29}$$

where δ is the noise level in $(0, 1)$, $\text{rand}(\text{size}(\vec{o}))$ is the Gaussian random noise with the same size as $\vec{o}$.

The precision of the approximation is characterized by the root mean-square error (rmse),

$$\text{rmse} = \sqrt{\frac{1}{M} \sum_{i=1}^{M} \frac{(\tau_{\text{comp}}(\lambda_i) - \tau_{\text{meas}}(\lambda_i))^2}{(\tau_{\text{comp}}(\lambda_i))^2}}, \tag{30}$$

which describes the average relative deviation of the retrieved signals from the true signals. In which, τ_{comp} refers to the retrieved signals, τ_{meas} refers to the measured signals.

In our example, the size distribution function $n_{\text{true}}(r)$ is given by

$$n_{\text{true}}(r) = 10.5 r^{-3.5} \exp(-10^{-12} r^{-2}).$$

The particle size radius interval of interest is $[0.1, 2]\,\mu\text{m}$. In the first place, the complex refractive index η is assumed to be $1.45 - 0.00i$. Then we invert the same data, supposing η has an imaginary part. The complex refractive index η is assumed to be $1.45 - 0.03i$ and $1.50 - 0.02i$, respectively. Numerical illustrations are plotted in Figs. 1–3 with noise levels $\delta = 0.005$, 0.01 and 0.05 for different refractive indices, respectively. The rmse's for each case are shown in Table 1. For finding the *a priori* information $\vec{n}_0$, we follow the algorithm described in Appendix C and choose the starting point for the primal–dual solution triplet as $(\vec{n}_1, \vec{z}_1, s_1) = (e_n, e_z, e_s)$, where e_n, e_z, e_s are column vectors corresponding to $\vec{n}_1$, $\vec{z}_1$, s_1 with components all unity. The iteration steps to get the *a priori* distribution for each case are shown in Table 2. For illustration of the normalized *a priori* distribution $\vec{n}_0$, we only plot it for the case $\eta = 1.45 - 0.00i$ and $\delta = 0.005$ (see Fig. 4 for details).
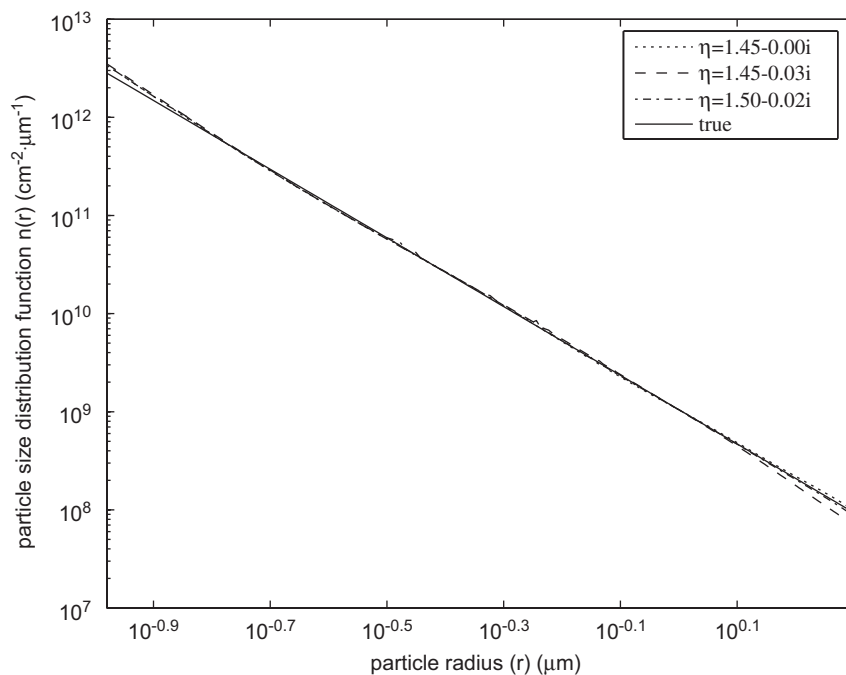
Fig. 2. Input and retrieved results with our inversion method in the case of error level $\delta = 0.01$ and different complex refractive indices.
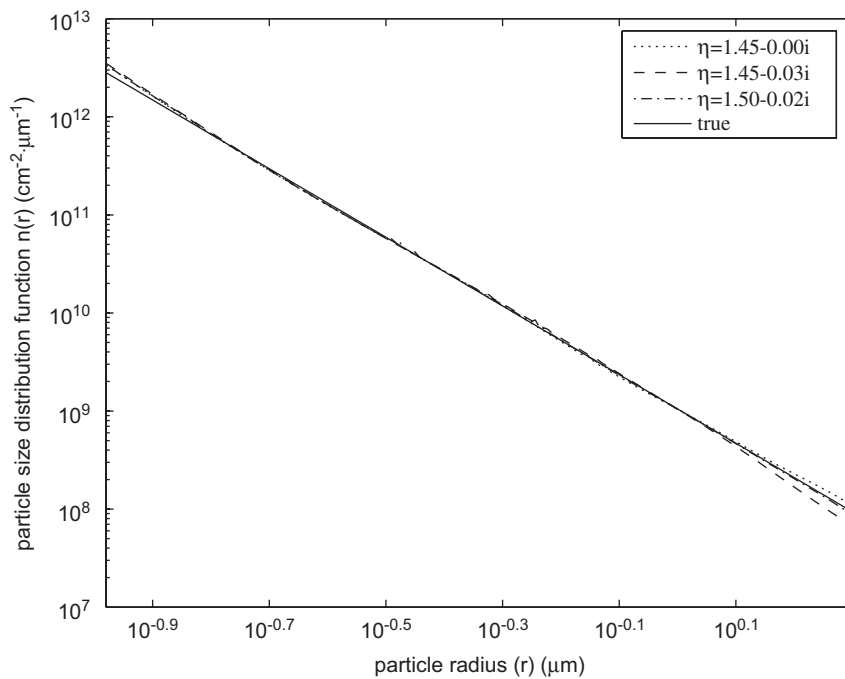

Fig. 3. Input and retrieved results with our inversion method in the case of error level $\delta = 0.05$ and different complex refractive indices.

Table 1
The root mean-square errors for different noise levels

Noise levels	$\eta = 1.45 - 0.00i$	$\eta = 1.45 - 0.03i$	$\eta = 1.50 - 0.02i$
$\delta = 0.005$	1.6443×10^{-4}	1.2587×10^{-4}	2.2773×10^{-4}
$\delta = 0.01$	1.6493×10^{-4}	1.2720×10^{-4}	2.2847×10^{-4}
$\delta = 0.05$	1.6996×10^{-4}	1.3938×10^{-4}	2.3504×10^{-4}

Table 2
The iteration steps for finding *a priori* information in different cases

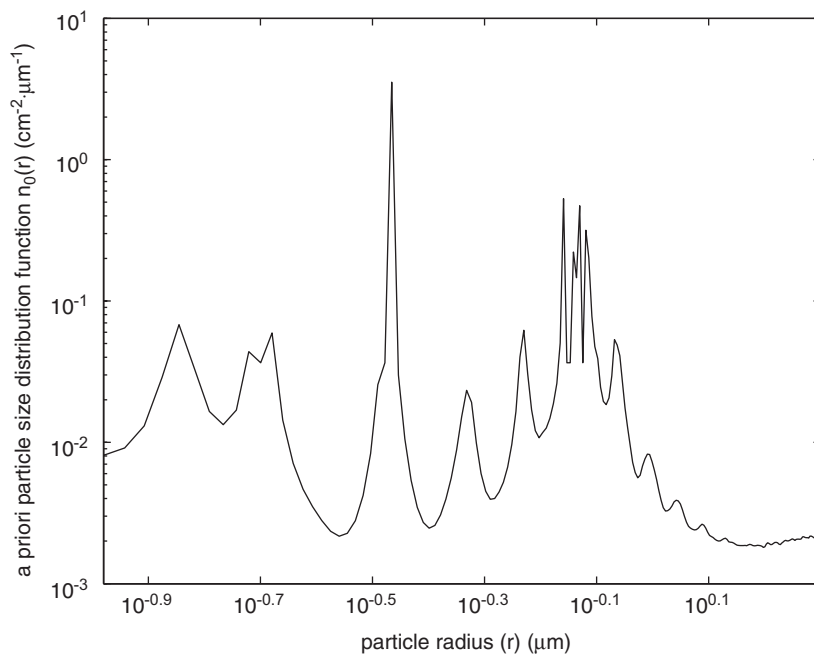| Noise levels	$\eta = 1.45 - 0.00i$	$\eta = 1.45 - 0.03i$	$\eta = 1.50 - 0.02i$
$\delta = 0.005$	17	13	16
$\delta = 0.01$	17	13	16
$\delta = 0.05$	17	13	16

Fig. 4. *A priori* particle size distribution n_0.

The proper choice of the *a priori* distribution $\vec{n}_0$ is very important for the success of the Gauss–Newton method. Without this information, the Gauss–Newton method may not converge to the right solution. For example, in our simulation, if we choose the starting point as $[0.1, 0.1, \ldots, 0.1]^{\mathrm{T}}$ and implement the method without considering this information, the algorithm diverges.

Our computer simulation method is not affected too much by the variation of the complex refractive index and noise. Therefore, our method is stable for retrieving aerosol particle size distribution functions.

5.2. Discussions on numerical results

We chose the ground-measured data by the Sun-photometer CE 318 (for illustration of the device, refer to Wang et al., 2006) to test the feasibility of the proposed algorithm. We have performed successive *in situ* experiments using
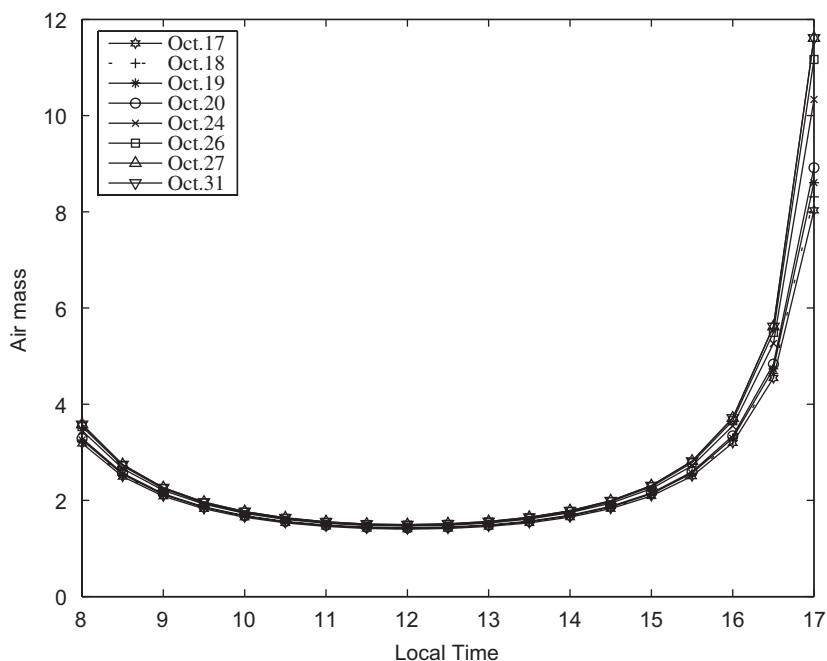
Fig. 5. The air mass variation at local time from October 17 to October 31, 2005.

the CE 318 from October 17 to October 31, 2005. The meteorological data was provided by the Ying Tan Agricultural Ecological Station of CERN (Chinese Ecosystem Research Network), which belongs to the Nanjing Institute of Soil Science of the Chinese Academy of Sciences.

Only the days October 17–20, 24, 26, 27 and 31 were used for aerosol inversion. The particle size in the range [0.1, 10] μm is examined. The days, October 17–20, were clean days with sunshine. The average wind speed was low, and the horizontal visibility was high. On October 24–30, the weather conditions varied frequently. But on those days, since the Sun-photometer CE 318 can track the sun and record the digital numbers (DNs), we also chose the AOT of those days to make inversion.

The air mass history from October 17 to October 31 is plotted in Fig. 5. It is shown that the air mass did not change too much at local time in different days and at the time from 8:00 in the morning to 16:00 in the afternoon, but varied rapidly from 16:00 to 17:00. We calculated the AOT at different wavelengths λ (μm), using the data measured in the afternoon on October 17–20, 24, 26, 27 and 31. The plots of the AOT variations with regard to the wavelength λ on these eight days are illustrated in Fig. 6. The slopes of the AOT variation are similar. It decreases with the increase of the wavelength. Evidently, the AOT can change at different times of a day. The magnitudes in these graphs indicate that the air is slightly polluted.

The climate of Yingtan is tropical/subtropical, and the wind system influences large climatic regions and reverses direction seasonally. The ground of the Yingtan Agricultural Ecological Station is mostly composed of red soil, so the atmospheric ferric oxide, iron hydroxide and sulfur depositions constitute the common particulates. From the meteorological data in the period October 17–31, we assume that the composition of the atmospheric aerosols consists of both small and large particles. Both the scattering and absorption of the particles play a major part. Therefore, a complex refractive index value of $\eta = 1.50 - 0.095i$ was used to perform the inversion. More detailed explanation can be found in Junge (1963), Weindisch and von Hoyningen-Huen (1994), and Reagan, Byrne, King, Spinhirne, and Herman (1980). In the numerical experiments, we chose the initial value α_0 of the regularization parameter as 0.1. Then, each α_k was iteratively calculated by the iteration formula given in Section 4.4. According to the regularization theory (Tikhonov & Arsenin, 1977; Xiao et al., 2003), when the computed solution approaches the true solution, the regularization parameters should approach the optimum value α^*, which should be a sufficiently small number. Our experiments also reveal this fact. The parameters α_k become sufficiently small (nearly zero) after successful iterations
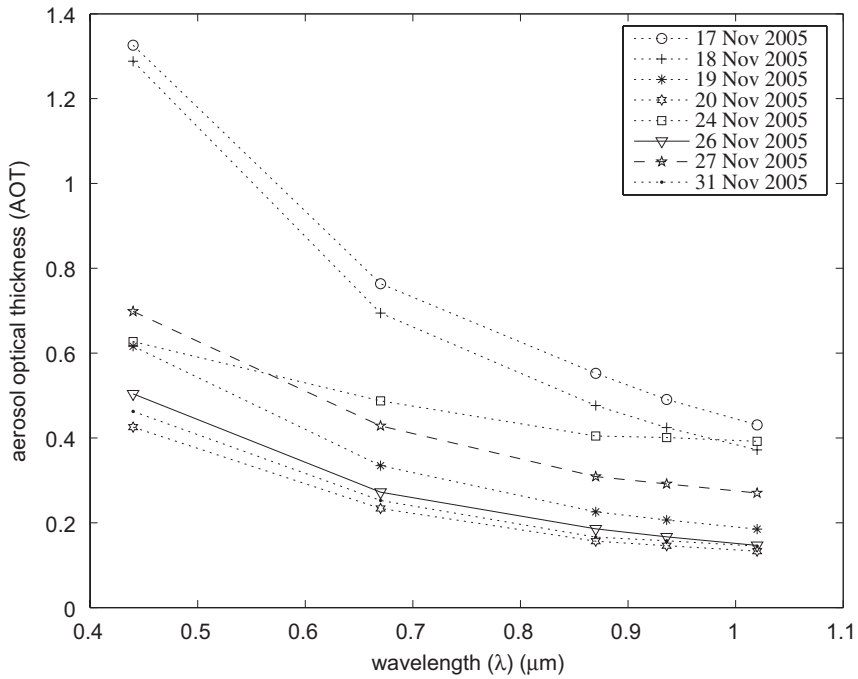
Fig. 6. Variation of aerosol optical thickness from October 17 to October 31 (PM), 2005.
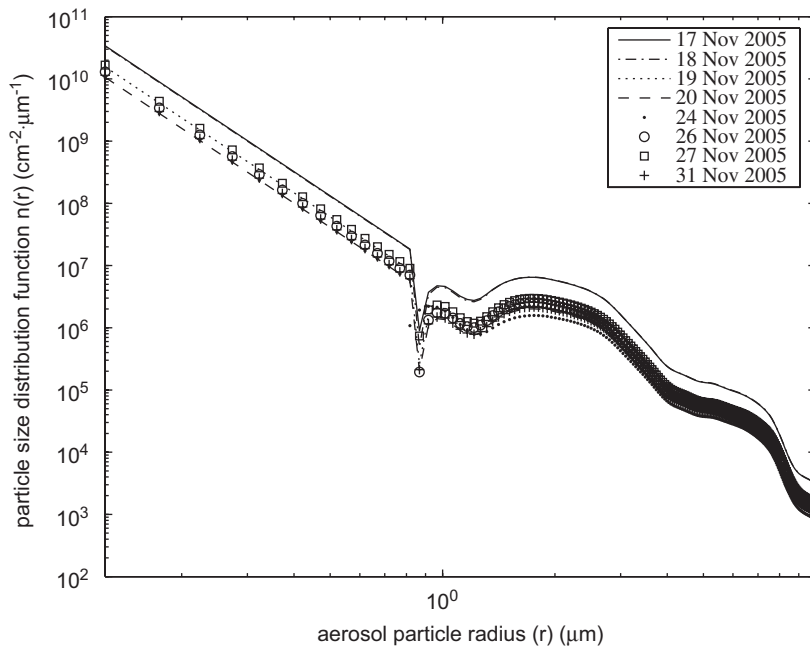

Fig. 7. Particle size distribution in October (PM), 2005.

in every measurement. By our algorithms, the retrieval results of the number of size distribution function $n(r)$ on October 17–31 are plotted in Fig. 7 for the chosen data in the afternoon. The figure indicates that the aerosol particles do not decrease rapidly. In all of the selected days, there are several oscillations of the particle size distribution function
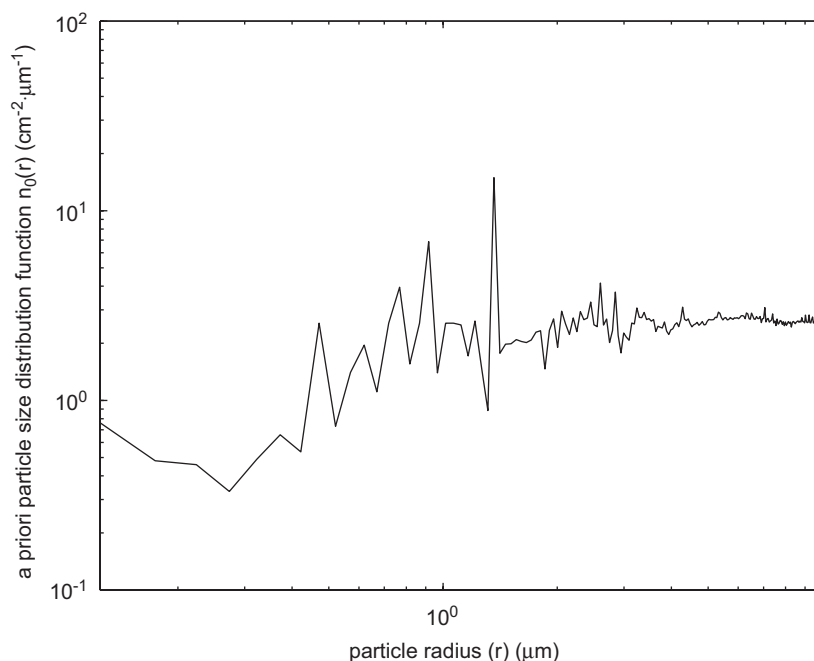
Fig. 8. *A priori* particle size distribution n_0 in October (PM), 2005.

near the radius 1.0 μm. Outside the region containing 1.0 μm, they change smoothly. For illustration of the normalized *a priori* distribution $\vec{n}_0$, see Fig. 8 for details. The number of iteration steps to get $\vec{n}_0$ is 11. From our experiments and the local environment observation, we conclude that the aerosol particle size distribution of Yingtan city is mainly small particles. The large particles of size 5–10 μm are mainly composed of ferric oxide, iron hydroxide and sulfur depositions. The results are consistent with the local air conditions and our observations.

6. Concluding remarks and future research

In this paper, we investigate the regularization methods for the solution of the atmospheric aerosol particle size distribution function retrieval. We reformulate the problem in functional space by introducing the first kind Fredholm integral equations, then the solution methods in l^1 and l^2 spaces are considered. The interior point solution method for finding an efficient *a priori* and regularized damped Gauss–Newton method for fast retrieval are proposed. We want to emphasis that there are different ways which can be developed to impose *a priori* information (Wang, 2007). For example, (P1) the unknowns $\vec{n}$ can be bounded. This method requires a good *a priori* upper bound for $\vec{n}$; (P2) applying different weights to the components of $\vec{n}$, then solve Eq. (6) under the constraint of the weights; (P3) imposing historical information on $\vec{n}$ provided that such historical information exists; (P4) simplifying the physical model by solving a l^p norm problem, which means the unknowns $\vec{n}$ can be obtained under the l^p scale.

We first did theoretical simulations to verify the feasibility of our inversion method. Our results show that the proposed method is quite stable and insensitive to complex refractive index η and noise levels.

Then, we applied our proposed method to the inversion of real extinction data obtained by adapting a commercial Sun-photometer CE 318. The numerical experiments illustrate that our new algorithm works well for the retrieval of aerosol particle size distribution functions.

Finally, we want to point out that our proposed method is also applicable to geophysical inverse problems and other research area in quantitative remote sensing (Bakushinsky & Goncharsky, 1994; Li & Wang, 1995; Wang, 2007). Our future research will investigate more robust regularization methods and develop new solution methods, and will do some numerical verifications based on ground-based remotely sensed data and satellite-based remotely sensed data in typical test area of China.

Appendix A. Conception of regularization

We saw in Section 3 that aerosol particle size distribution function inversion problem can be formulated as operator equations of the form

$$Kn = o, \tag{A.1}$$

where K is a linear compact operator between Hilbert spaces F and O.

A regularization strategy is a family of linear and bounded operators

$$\Pi^\alpha : O \to F, \quad \alpha > 0, \tag{A.2}$$

such that

$$\Pi^\alpha Kn = n \quad \text{for all } n \in F, \tag{A.3}$$

i.e., the operators $\Pi^\alpha K$ converge pointwise to the identity.

Refer to our method, the Π^α is defined as

$$\Pi^\alpha = (K^* K + \alpha L)^{-1} K^*, \tag{A.4}$$

where L is a pre-assigned operator, K^* is the adjoint operator of K, $\alpha \in (0, 1)$.

Appendix B. Conception of *a priori* information

By minimizing

$$\tfrac{1}{2} \| Kn - o \|^2 + \tfrac{1}{2} \alpha \| L^{1/2} n \|^2 \tag{B.1}$$

we obtain

$$n^\alpha = \Pi^\alpha o. \tag{B.2}$$

Let us consider a different form of the minimization problem

$$\min\{ \tfrac{1}{2} \| Kn - o \|^2 + \alpha \Omega(n - n_0) : n \in F \}, \tag{B.3}$$

where n_0 is the trial solution, $\alpha > 0$ is the regularization parameter and Ω is the stabilizing functional.

The *a priori* information/knowledge refers to how to choose the stabilizing functional Ω and the trial solution n_0, which is an information (or restrictions) about smoothness of a solution and give regularization algorithm which approximate the normal solution of Eq. (A.1).

The *a priori* information is quite important for obtaining a stable solution and accelerating the convergence rate of the algorithm.

Refer to our method, the *a priori* is: (1) choosing n_0 by solving an l^1 norm problem in l^1 space; (2) applying regularization algorithm in l^2 space.

Appendix C. Computing an *a priori* by searching for an interior point solution

The *a priori* in this section refers to choosing n_0 by solving an l^1 norm problem in l^1 space.

The algorithm described in Section 4.1 is a special case of the constrained linear programming problem

$$\min c^{\mathrm{T}}\vec{n} \quad \text{subject to } \mathscr{K}\vec{n} = \vec{d}, \ \vec{n} \geqslant 0, \tag{C.1}$$

where $\vec{n}$ is a vector of N variables. The dual problem of (C.1) is

$$\max \vec{d}^{\mathrm{T}}\vec{z} \quad \text{subject to } \mathscr{K}^{\mathrm{T}}\vec{z} + s = c, \ s \geqslant 0. \tag{C.2}$$

To solve this problem, we consider the logarithmic barrier problem parameterized by the positive barrier parameter μ:

$$\min c^{\mathrm{T}}\vec{n} - \mu \sum_{j=1}^{N} \log(n_j) \quad \text{subject to } \mathscr{K}\vec{n} = \vec{d}, \ \vec{n} \geqslant 0. \tag{C.3}$$

The barrier function satisfies

$$\lim_{n_j \to 0} -\mu \log(n_j) = \infty. \tag{C.4}$$

If $\vec{n} > 0$ initially, then barrier function maintains $\vec{n} > 0$. Define optimality conditions for barrier problem

$$L(\vec{n}, \vec{z}) = c^{\mathrm{T}}\vec{n} - \mu \sum_{j=1}^{N} \log(n_j) - \vec{z}^{\mathrm{T}}(\mathscr{K}\vec{n} - \vec{d}). \tag{C.5}$$

Differentiation gives

$$\frac{\partial L}{\partial n_j} = c_j - \mu n_j^{-1} - \mathscr{K}_{:j}^{\mathrm{T}}\vec{z}, \quad \frac{\partial L}{\partial z_i} = \vec{d}_i - \mathscr{K}_{i:}\vec{n}, \tag{C.6}$$

where $\mathscr{K}_{:j}$ means the jth column of $\mathscr{K}$, $\mathscr{K}_{i:}$ means the ith row of $\mathscr{K}$. The above expression can be simply written as matrix–vector form

$$\mathrm{grad}_{\vec{n}} L(\vec{n}, \vec{z}) = c - \mu D^{-1}e - \mathscr{K}^{\mathrm{T}}\vec{z}, \quad \mathrm{grad}_{\vec{z}} L(\vec{n}, \vec{z}) = \vec{d} - \mathscr{K}\vec{n}, \tag{C.7}$$

where

$$D = \begin{bmatrix} n_1 & 0 & \cdots & 0 \\ 0 & n_2 & \cdots & 0 \\ \vdots & \vdots & \ddots & \vdots \\ 0 & 0 & \cdots & n_N \end{bmatrix}. \tag{C.8}$$

This yields the Karush–Kuhn–Tucker conditions

$$\mathscr{K}^{\mathrm{T}}\vec{z} = c - \mu D^{-1}e, \quad \mathscr{K}\vec{n} = \vec{d}, \quad \vec{n} > 0. \tag{C.9}$$

If we define $s = \mu D^{-1}e$, we have the optimality conditions

$$\mathscr{K}^{\mathrm{T}}\vec{z} + s = c, \quad \mathscr{K}\vec{n} = \vec{d}, \quad Ds = \mu e, \quad \vec{n} > 0. \tag{C.10}$$

A feasible solution $(\vec{n}, \vec{z}, s)^{\mathrm{T}}$ to this system is both primal feasible, i.e., $\vec{n} \in S_p = \{\vec{n} : \mathscr{K}\vec{n} = \vec{d}, \vec{n} > 0\}$ and dual feasible, i.e., $(\vec{z}, s) \in S_D = \{(\vec{z}, s) : \mathscr{K}^{\mathrm{T}}\vec{z} + s = c, s = \mu D^{-1}e > 0\}$.

Considering the dual gap $c^T\vec{n} - \vec{d}^T\vec{z} = \vec{n}^T s = \mu N$, therefore, numerically, we solve a nonlinear equation

$$F(\vec{n}, \vec{z}, s) = \begin{bmatrix} \mathcal{K}\vec{n} - \vec{d} \\ \mathcal{K}^T\vec{z} + s - c \\ Ds - \beta\mu e \end{bmatrix} = \begin{bmatrix} 0 \\ 0 \\ 0 \end{bmatrix}, \tag{C.11}$$

where β is the damping parameter in $[0, 1]$.

Assume that $(\vec{n}_k, \vec{z}_k, s_k)^T$ is given, then one iteration of Newton method to $F(\vec{n}, \vec{z}, s) = 0$ yields

$$\operatorname{grad} F(\vec{n}_k, \vec{z}_k, s_k) \begin{bmatrix} d_{\vec{n}} \\ d_{\vec{z}} \\ d_s \end{bmatrix} = -F(\vec{n}_k, \vec{z}_k, s_k). \tag{C.12}$$

Since

$$\operatorname{grad} F(\vec{n}_k, \vec{z}_k, s_k) = \begin{bmatrix} \mathcal{K} & 0 & 0 \\ 0 & \mathcal{K}^T & I \\ S_k & 0 & D_k \end{bmatrix}, \tag{C.13}$$

we obtain

$$\begin{bmatrix} \mathcal{K} & 0 & 0 \\ 0 & \mathcal{K}^T & I \\ S_k & 0 & D_k \end{bmatrix} \begin{bmatrix} d_{\vec{n}} \\ d_{\vec{z}} \\ d_s \end{bmatrix} = \begin{bmatrix} \vec{d} - \mathcal{K}\vec{n}_k \\ c - \mathcal{K}^T\vec{z}_k - s_k \\ -D_k s_k + \beta\mu_k e \end{bmatrix}. \tag{C.14}$$

We give the algorithm as follows:

Algorithm (*Computing an interior point solution*).

(1) Initialization: choose $(\vec{n}_1, \vec{z}_1, s_1)^T$ with $\vec{n}_1, \vec{z}_1 > 0$, and three tolerances $\varepsilon_{\vec{n}}, \varepsilon_{\vec{z}}, \varepsilon_s > 0$;
(2) Iteration: for k from 1 to ∞;
(3) Calculate the residuals

$$r_{\vec{n}}^k = \vec{d} - \mathcal{K}\vec{n}_k,$$

$$r_{\vec{z}}^k = c - \mathcal{K}^T\vec{z}_k - s_k,$$

$$\mu_k = \frac{1}{N}\vec{n}_k^T s_k;$$

(4) If $\|r_{\vec{n}}^k\| \leqslant \varepsilon_{\vec{n}}$, $\|r_{\vec{z}}^k\| \leqslant \varepsilon_{\vec{z}}$, $\|\mu_k\| \leqslant \varepsilon_s$, Stop;
(5) Choose $\beta \in (0, 1)$ and solve (C.14);
(6) Compute

$$\tau^{\max} = \operatorname{argmax}_{\tau \geqslant 0}\left\{ \begin{bmatrix} \vec{n}_k \\ s_k \end{bmatrix} + \tau \begin{bmatrix} d_{\vec{n}} \\ d_s \end{bmatrix} \geqslant 0 \right\}; \tag{C.15}$$

(7) For some $\theta \in (0, 1)$, set

$$\tau := \min\{\theta\tau^{\max}, 1\};$$

(8) Update

$$\vec{n}_{k+1} := \vec{n}_k + \tau d_{\vec{n}},$$

$$\vec{z}_{k+1} := \vec{z}_k + \tau d_{\vec{z}},$$

$$s_{k+1} := s_k + \tau d_s.$$

Example (*Computing an interior point solution*).   To clearly present our method, we give a specific calculation example, which is a constrained minimization problem

$$\min -1n_1 - 2n_2 \quad \text{subject to } n_1 + n_2 = 1, \quad n_1, n_2 \geqslant 0. \tag{C.16}$$

If we set $\vec{n} = [n_1 \ n_2]^T$, $c = [-1 \ -2]^T$, $\mathscr{K} = [1 \ 1]$, $\vec{d} = 1$, then following the above mentioned steps, we have

$$F(\vec{n}, \vec{z}, s) = \begin{bmatrix} \mathscr{K}\vec{n} - \vec{d} \\ \mathscr{K}^T\vec{z} + s - c \\ Ds - \beta\mu e \end{bmatrix} = \begin{bmatrix} 0 \\ 0 \\ 0 \end{bmatrix}, \tag{C.17}$$

where $\vec{z} = [z_1 \ z_2]^T$, $s = [s_1 \ s_2]^T$, $D = \text{diag}(n_1, n_2)$, $\mu = \frac{1}{2}\vec{n}^T s$, $e = [1 \ 1]^T$, $\beta = 0.1$ is the damping parameter in $[0, 1]$. It is easy to identify

$$\text{grad } F(\vec{n}_k, \vec{z}_k, s_k) = \begin{bmatrix} 1 & 1 & 0 & 0 & 0 \\ 0 & 0 & 1 & 1 & 0 \\ 0 & 0 & 1 & 0 & 1 \\ s_1 & 0 & 0 & \vec{n}_1 & 0 \\ 0 & s_2 & 0 & 0 & \vec{n}_2 \end{bmatrix}.$$

Therefore, following the above algorithm, we obtain after seven iteration steps: the solution is $\vec{n}^* = [0.0000 \ 1.0000]^T$, the dual gap is $s^T\vec{n}^* = 1.0042e - 007$, the minimization value of the object function is $c^T\vec{n}^* = -2.0000$.

Appendix D. Damped Gauss–Newton method with line search

Consider the minimization problem

$$\min J[\vec{n}] := \frac{1}{2}\|R(\vec{n})\|^2. \tag{D.1}$$

The Gauss–Newton method computes a step $s_k = \vec{n}_{k+1} - \vec{n}_k$ by solving the minimum norm of the linear least squares problem

$$\min \frac{1}{2}\|R(\vec{n}_k) + R'(\vec{n}_k)s\|^2, \tag{D.2}$$

which leads to $s_k = -H^{-1}g_k$ and $\vec{n}_{k+1} = \vec{n}_k + s_k$.

The damped Gauss–Newton method refers to a line search technique being used to determine a descent direction (Nocedal & Wright, 1999), i.e., finding a damping parameter γ_k and deciding how far to move along this direction,

$$s_k = -\gamma_k H^{-1}g_k. \tag{D.3}$$

In computing the damping parameter γ_k, we face a tradeoff. We would like to choose γ_k to give a substantial reduction of J, but at the same time, we do not want to spend too much time making the choice. A popular inexact line search condition stipulates that γ_k should first of all give sufficient decrease in the objective function J, as measured by the following inequality:

$$J(\vec{n}_k + \gamma_k s_k) \leqslant J(\vec{n}_k) + c_1\gamma_k g_k^T s_k, \tag{D.4}$$

for some constant $c_1 \in (0, 1)$.

The sufficient decrease condition is not enough by itself to ensure that the algorithm makes reasonable progress, because it is satisfied for all sufficiently small values of γ. To rule out unacceptably short steps we introduce a second requirement, which requires γ_k to satisfy

$$g(\vec{n}_k + \gamma_k s_k)^T s_k \geqslant c_2 g_k^T s_k, \tag{D.5}$$

for some constant $c_2 \in (c_1, 1)$, where c_1 is the constant from (D.4).

Conditions (D.4)–(D.5) are called Wolfe conditions. In our algorithm, we chose $c_1 = 0.1$ and $c_2 = 0.4$.

References

Ångström, A. (1929). On the atmospheric transmission of sun radiation and on dust in the air. *Geografiska Annaler*, *11*, 156–166.

Bakushinsky, A., & Goncharsky, A. (1994). *Ill-posed problems: Theory and applications*. Dordrecht: Kluwer Academic Publishers.

Bockmann, C. (2001). Hybrid regularization method for the ill-posed inversion of multiwavelength lidar data in the retrieval of aerosol size distributions. *Applied Optics*, *40*, 1329–1342.

Bohren, G. F., & Huffman, D. R. (1983). *Absorption and scattering of light by small particles*. New York: Wiley.

Chahine, M. T. (1970). Inverse problems in radiation transfer: Determination of atmospheric parameters. *Journal of Aerosol Science*, *27*, 960–967.

Davies, C. N. (1974). Size distribution of atmospheric aerosol. *Journal of Aerosol Science*, *5*, 293–300.

Ferri, F., Bassini, A., & Paganini, E. (1995). Modified version of the Chahine algorithm to invert spectral extinction data for particle sizing. *Applied Optics*, *34*, 5829–5839.

Heintzenberg, J. (1994). Properties of log-normal particle size distributions. *Aerosol Science and Technology*, *21*, 46–48.

Junge, C. E. (1963). *Air chemistry and radioactivity*. New York: Academic Press.

King, M. D., Byrne, D. M., Herman, B. M., & Reagan, J. A. (1978). Aerosol size distributions obtained by inversion of spectral optical depth measurements. *Journal of Aerosol Science*, *35*, 2153–2167.

Li, X., & Wang, J. (1995). *Vegetation optical remote sensing model and vegetation structural parameterization*. Beijing: Science Press.

Lumme, K., & Rahola, J. (1994). Light scattering by porous dust particles in the discrete-dipole approximation. *The Astrophysical Journal*, *425*, 653–667.

Mccartney, G. J. (1976). *Optics of atmosphere*. New York: Wiley.

Nguyen, T., & Cox, K. (1989). A method for the determination of aerosol particle distributions from light extinction data. In *Abstracts of the American association for aerosol research annual meeting* (p. 330). Cincinnati, Ohio: American Association of Aerosol Research.

Nocedal, J., & Wright, S. J. (1999). *Numerical optimization*. New York: Springer.

Phillips, D. L. (1962). A technique for the numerical solution of certain integral equations of the first kind. *Journal of the Association for Computing Machinery*, *9*, 84–97.

Ramachandran, G., Leith, D., & Todd, L. (1994). Extraction of spatial aerosol distribution from multispectral light extinction measurements with computed tomography. *Journal of the Optical Society of America A*, *11*, 144–154.

Reagan, A. J., Byrne, D. M., King, D. M., Spinhirne, J. D., & Herman, B. M. (1980). Determination of complex refractive index and size distribution of atmospheric particles from bistatic–monostatic Lidar and solar radiometer measurements. *Journal of Geophysical Research*, *85*, 1591–1599.

Shifrin, K. S., & Zolotov, L. G. (1996). Spectral attenuation and aerosol particle size distribution. *Applied Optics*, *35*, 2114–2124.

Tikhonov, A. N., & Arsenin, V. Y. (1977). *Solutions of ill-posed problems*. New York: Wiley.

Twomey, S. (1963). On the numerical solution of Fredholm integral equations of the first kind by the inversion of the linear system produced by quadrature. *Journal of the Association for Computing Machinery*, *10*, 97–101.

Twomey, S. (1975). Comparison of constrained linear inversion and an iterative nonlinear algorithm applied to the indirect estimation of particle size distributions. *Journal of Computational Physics*, *18*, 188–200.

Twomey, S. (1977). *Atmospheric aerosols*. Amsterdam: Elsevier Science Publishing Company.

Voutilainenand, A., & Kaipio, J. P. (2000). Statistical inversion of aerosol size distribution data. *Journal of Aerosol Science*, *31*(Suppl. 1), 767–768.

Wang, Y. F. (2007). *Computational methods for inverse problems and their applications*. Beijing: Higher Education Press.

Wang, Y. F., Fan, S. F., Feng, X., Yan, G. J., & Guan, Y. N. (2006). Regularized inversion method for retrieval of aerosol particle size distribution function in $W^{1,2}$ space. *Applied Optics*, *45*, 7456–7467.

Weindisch, M., & von Hoyningen-Huen, W. (1994). Possibility of refractive index determination of atmospheric aerosol particles by ground-based solar extinction and scattering measurements. *Atmospheric Environment*, *28*, 785–792.

Wright, D. L. (2000). Retrieval of optical properties of atmospheric aerosols from moments of the particle size distribution. *Journal of Aerosol Science*, *31*, 1–18.

Wright, D. L., Yu, S. C., Kasibhatla, P. S., McGraw, R., Schwartz, S. E., Saxena, V. K. et al. (2002). Retrieval of aerosol properties from moments of the particle size distribution for kernels involving the step function: Cloud droplet activation. *Journal of Aerosol Science*, *33*, 319–337.

Xiao, T. Y., Yu, Sh. G., & Wang, Y. F. (2003). *Numerical methods for the solution of inverse problems*. Beijing: Science Press.

Yamamoto, G., & Tanaka, M. (1969). Determination of aerosol size distribution function from spectral attenuation measurements. *Applied Optics*, *8*, 447–453.

Ye, M., Wang, S., Lu, Y., Hu, T., Zhu, Z., & Xu, Y. (1999). Inversion of particle-size distribution from angular light-scattering data with genetic algorithms. *Applied Optics*, *38*, 2677–2685.

Ye, Y. (1997). *Interior point algorithms: Theory and analysis. Wiley-interscience series in discrete mathematics and optimization*. New York: Wiley.